Demography (2022) 59(6):2109–2134 Published online: 3 November 2022
DOI 10.1215/00703370-10286336

A Unified Model of Cohort Mortality

Adriana Lleras-Muney and Flavien Moreau

ABSTRACT We propose a dynamic production function of population health and mortality from birth onward. Our parsimonious model provides an excellent fit for the mortality and survival curves for primate and human populations since 1816. The model sheds light on the dynamics behind many phenomena documented in the literature. Simple extensions of the model can reproduce (1) the existence and evolution of mortality gradients across socioeconomic statuses documented in the literature, (2) nonmonotonic dynamic effects of *in utero* shocks, (3) persistent or scarring effects of wars, and (4) mortality displacement after large temporary shocks, such as extreme weather.

KEYWORDS Mortality • Health • *In utero* shocks • Selection • Scarring

Introduction

We propose a coherent framework to understand how population health and mortality evolve from birth onward and how economic and other environmental factors throughout life affect this evolution. Statistical and economic models of health and mortality typically concentrate on adults. Yet, a large literature has documented that events and investments *in utero* and throughout childhood are powerful predictors of later-life economic and health outcomes (Almond and Currie 2011; Almond et al. 2018). In the absence of such a quantitative model, it is difficult to predict how shocks will affect population health at various ages, and it is even harder to design optimal investment or compensation policies.

We present a simple dynamic model of the production of health from birth to death for a heterogeneous population. In the spirit of classic demographic work (Vaupel et al. 1979), some individuals are born frailer than others. Subsequently, the distribution among survivors evolves according to a simple law of motion that depends on the level of external resources, which are stochastic. As in Grossman's (1972) classic work on the production of health, an individual's health deteriorates with age but can increase with investments. At any age, individuals in poor health die. In addition, individuals die from reasons unrelated to their health status. During the adolescent years, these external causes of death account for a large portion of deaths.

We estimate this model separately for more than 100 birth cohorts born since 1816, using high-quality data from the Human Mortality Database (2017). Despite substantial changes in life expectancy throughout the period, the model provides an

ELECTRONIC SUPPLEMENTARY MATERIAL The online version of this article (https://doi.org/10.1215/00703370-10286336) contains supplementary material.

excellent characterization of the mortality age profiles for each cohort and is consistent with two stylized facts: (1) the profile of log mortality rates by age has a J-shape; and (2) survival curves for humans have rectangularized over the last two centuries, flattening throughout life and dropping abruptly at older ages.

We then show that simple extensions of the model can generate other previously documented phenomena. Specifically, we show that (1) changes in lifetime resources generate socioeconomic status (SES) gradients (persistent gaps in log mortality rates across populations with different SES) that fall with age; (2) *in utero* insults result in nonmonotonic impacts on health and mortality over the lifetime; (3) short-term negative shocks (e.g., wars) that temporarily lower resources result in scarring (elevated mortality of survivors); and (4) environmental shocks (e.g., hot weather) that affect the threshold for dying lead to harvesting (temporarily elevated mortality followed by temporarily lower mortality). The model also describes the evolution of chimpanzee mortality well.

The evolution of mortality over the lifetime is, in fact, remarkably similar across human populations and across most primates. Because of this regularity, demographers have searched for a "unified" model of mortality that would predict mortality from birth to death at least since the early nineteenth century (Carnes et al. 1996). Like much of the literature that followed (e.g., Li and Anderson 2013), Gompertz's (1825) model accounts for mortality *only after a certain age*, focusing on the roughly log-linear portion of the mortality curve after age 40. There are a few exceptions. A popular model by Heligman and Pollard (1980) fits period data mortality rates from various contexts remarkably well. More recent demographic models describe aggregate mortality rates as a function of various parameters, albeit with different objectives: Sharrow and Anderson (2016) decomposed the gains in longevity into intrinsic and extrinsic deaths, whereas Palloni and Beltrán-Sánchez (2017) simulated the effects of childhood frailty on mortality throughout life.

Our first contribution to the literature (reviewed in detail in online appendix B) is to provide a new model of cohort mortality. Our approach differs in one fundamental aspect from the demographic approach just described. As in the seminal Grossman (1972) model, we model directly how the health stock of each *individual* evolves, rather than modeling the mortality or survival rates of only the aggregate population. Like Sharrow and Anderson (2016), we decompose mortality into two separate causes of death: extrinsic and intrinsic. Like Palloni and Beltrán-Sánchez (2017), we use our model to study the effects of frailty. Our model accomplishes both aims within the same framework while achieving a great fit like Heligman and Pollard's (1980) model does.

The second contribution of this paper is to show that simple modifications of this baseline model account for a wide range of existing demographic phenomena. We demonstrate this by studying the effects of increasing lifetime resources and the impact of negative *in utero* shocks on a population's subsequent average health and mortality. We also study the effects of temporary shocks, such as wars and bad weather. To our knowledge, no other model both provides an excellent fit to the cohort data and can also explain the variety of phenomena we study.

Our model provides a framework that bridges the demographic and economic approaches: we model individual health as economists do, but we study its aggregate implications for population mortality in the tradition of demographic studies. Our model is more parsimonious than Grossman's (1972) classic work or its most recent successors in the economics literature (Dalgaard and Strulik 2014; Galama and van

Kippersluis 2019). These more complex models were developed to understand health expenditures and health behaviors. We focus only on a production process and are silent about maximizing behavior, at least initially.

Our main innovation relative to economic models is to include childhood. Alternative state-of-the-art models, such as Dalgaard and Strulik's (2014) accumulating health deficits model or Galama and van Kippersluis's (2019) theory of SES and mortality, start with adults. A recent model by Dalgaard et al. (2021) includes childhood, but it does so by adding a separate health production function for childhood. Instead, our framework describes aging from birth to death with a unique law of motion, where mortality declines during childhood owing to both selection and investments. We also demonstrate that our model fits mortality curves for entire cohorts well, which economic models have not demonstrated.

Stylized Facts: Health and Mortality Over the Lifetime

Mortality

We study the evolution of mortality for a given cohort using data from the Human Mortality Database (HMD; 2017). The HMD provides population and death counts by age, birth year, and gender collected through vital registration systems (birth and death certificates) and censuses from 1816 to 2015. Despite a few limitations, the HMD is the highest quality data available for cohort analysis. We compute mortality rates by age for each cohort as the number of deaths divided by the population at that age, and we use these rates to compute survival rates and life expectancy (see online appendix D). We focus on French cohorts for two reasons: these cohorts are large, and the data extend back to 1816.

We study cohort mortality rates, which are used more often than period rates. In a stationary environment, with stable mortality rates by age over time, the two are very close, but they diverge otherwise. The evolution of period and cohort life expectancy at birth by gender in France is summarized in Figure A10 (this and all other figures and tables designated with an "A" are shown in the online appendix).[1] For the 1816–1860 cohorts, (cohort and period) life expectancy at birth was stable at approximately age 40 for females and age 39 for males. However, life expectancy increased in the late nineteenth century, with cohort life expectancy rising more than period life expectancy. Several cohorts of men (born in roughly 1880–1900) experienced declines in life expectancy, likely as a result of World War I and World War II. Among those born around 1920, females and males lived approximately 69 and 59 years, respectively—substantially longer than cohorts born a century earlier.

Figure 1 shows the logarithm of mortality rates by age for selected birth cohorts of women born between 1860 and 1940. Results for various European countries are shown in panel a, and results for France are shown in panel b. Although the level of

[1] Period life expectancy is computed using the cross-sectional mortality rates of all cohorts alive in a year, whereas cohort life expectancy is computed using a cohort's *realized* mortality rates. For example, 1850 period life expectancy uses the observed mortality rates of 70-year-olds in 1850. But when 1850 cohort life expectancy is computed, the mortality rates at age 70 are those observed in 1920.

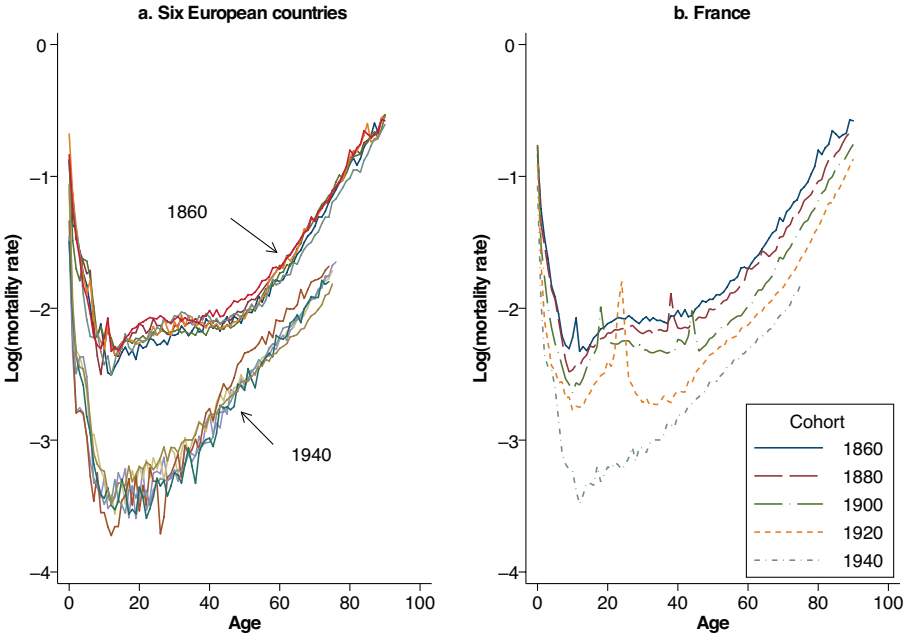

Fig. 1 Cohort mortality rates for selected European cohorts born in 1860–1940. Data are from the Human Mortality Database (2017). Panel a shows the $\log_{10}$ of the mortality rates, by age, for women born in 1860 and in 1940 in six European countries (Belgium, Denmark, the Netherlands, Sweden, France, and Norway). Panel b shows the mortality rates for women born in France in 1860, 1880, 1900, 1920, and 1940.

mortality changed substantially over time, the basic evolution of mortality rates by age is similar across many countries and periods.

For a given cohort, the logarithm of mortality has the shape of a check mark: high at birth, low among the young, and high and rising almost linearly with age in adulthood. Mortality curves also display an "adolescent hump," especially visible for cohorts born in the nineteenth century: starting in adolescence, mortality rates increase rapidly (Preston et al. 2000; Thiele 1871). Finally, spikes are evident for some cohorts, corresponding to wars and epidemics. These patterns are more visible when examining all the cohort curves, which are similar but not identical for men (see Figures A11 and A12). These patterns are not unique to humans. Bronikowski et al. (2011) used longitudinal data from primates living in the wild and showed that these mortality patterns are similar across all primates.

Health

The World Health Organization defines health as "a state of complete physical, mental and social well-being and not merely the absence of disease and infirmity."[2] Thus,

[2] See https://www.who.int/about/governance/constitution.

health is a multidimensional concept that is not easily captured by any single metric, but partial measures are available. A striking empirical pattern is that the distribution of various health indicators observed at different ages is roughly Gaussian. For example, the distribution of birth weights is normal (Wilcox and Russell 1983), and so is the distribution of adult heights (Tanner 1981).

How does the distribution of health evolve with age? Unfortunately, the HMD does not contain any health measures. In fact, we are not aware of any data that track a consistent measure of health from birth to death for a given cohort. But several studies provide partial descriptions of this evolution. Mean health increases and then falls with age, peaking sometime in young adulthood. Biological functions, such as muscle mass (Metter et al. 1999), bone mass (Baxter-Jones et al. 2011), and performance in physical and cognitive tasks (Allen and Hopkins 2015; Strittmatter et al. 2020), peak sometime between ages 20 and 35. Self-reported measures of health, which capture overall health, decline in adulthood (Case and Deaton 2005; Deaton and Paxson 1998; Halliday et al. 2018; Kaestner et al. 2020).

The variance in health also rises with age and then seems to level off or fall among the oldest, although the data are less clear about what happens among the oldest (Deaton and Paxson 1998; Halliday et al. 2019; Halliday 2011). The variance in organ function also rises with age (Steves et al. 2012). Lastly, both objective measures of health and subjective overall measures of health are strong predictors of mortality (Benyamini and Idler 1999; McGee et al. 1999).

A Unified Model of Aging and Mortality

In this section, we present a simple model that can account for these basic stylized facts about health and mortality.

Individuals are born with an initial health endowment, H_0, that differs across individuals in the population and has an unknown distribution.[3] Every period, the environment provides resources (I) to all individuals, which increase health (H). In this basic model (and in contrast to Grossman's), individuals have no control over their resources. In addition, individuals in the same environment are more or less lucky and experience an idiosyncratic shock (ε_a) to their resources. For example, I characterizes the per capita amount of food that a country produces, but a given person might receive less if, for instance, rainfall was unusually low in their location. The variance of ε_a captures how unequal the distribution of resources is. These idiosyncratic shocks are assumed to be independent and identically distributed every period.

Finally, the health stock depreciates each period by an amount $d(a)$, which increases with age a ($d'(a) > 0$). This aging process reflects "the accumulation of random damage to the building blocks of life—especially to DNA, certain proteins, carbohydrates, and lipids (fats)—that begins early in life and eventually exceeds the

[3] Although health is multidimensional, we use a single index, as in Grossman (1972). This health measure can be viewed as a sufficient statistic for a larger collection of health indicators (e.g., vascular, brain functions), each following a different law of motion. Alternatively, one could model various health dimensions and how each affects the probability of dying, as in engineering models of aging or competing-risks models.

body's self-repair capabilities" (Olshansky et al. 2002:93). These forces determine the evolution of the health stock, which is an unobserved latent variable.

Individuals die when their stock of health dips below a threshold $\underline{H}$, which is fixed throughout the lifetime and identical for all individuals. (This assumption that overall health predicts mortality is consistent with empirical observations: for example, self-reported heath and objective measures of health both predict mortality (Ganna and Ingelsson 2015; Idler and Benyamini 1997).) Let $D_a = \mathbb{I}\left(H_a \leq \underline{H}, D_{a-1} = 0\right)$ denote the random variable equal to 1 if the individual dies at age a. Then, the population's health and mortality are characterized by the following dynamic system:

$$\begin{cases} H_a = H_{a-1} - d\left(a\right) + I + \varepsilon_a \text{ if } D_{a-1} = 0 \\ D_a = \mathbb{I}\left(H_a \leq \underline{H}, D_{a-1} = 0\right) \\ D_0 = 0, \end{cases}$$

with $I \in \mathbb{R}$. Note that if $D_a = 1$, then H_a is undefined; individuals' health is not observed after they die. But we observe the mortality rate for the population at age a, which is given by $MR_a = \mathbb{P}\left(D_a = 1 \mid D_s = 0, \forall s < a\right)$. Thus, the distribution of health and the mortality rate at any age are functions of the entire history of shocks and investments. We make three key parametric assumptions to make the model more tractable and consistent with the empirical evidence above. First, H_0 follows a normal distribution $\mathcal{N}\left(\mu_H, \sigma^2\right)$. Second, shocks to resources every period also follow a normal distribution, $\varepsilon_a \sim \mathcal{N}\left(0, \sigma^2\right)$.[4] Third, depreciation is a power function, $d\left(a\right) = \delta a^{\alpha}$ with $\delta \in \left(0, \infty\right)$, $\alpha \in \left(0, \infty\right)$.[5] This aging process starts slowly at birth, consistent with evidence that aging markers deteriorate among children (Wong et al. 2010). It increases rapidly with age among adults, as in biological models of senescence (Armitage and Doll 1954; Pompei and Wilson 2002).[6]

Figure 2 illustrates the evolution of health and mortality in the first two periods. Initially, the health distribution is normal. Then it shifts to the right during the first period as long as I is positive (and larger than the aging term) and spreads out (because of the stochastic shock, ε_a). Individuals who were born too frail or experienced large negative shocks move to the left of the threshold and die. Graphically, the infant mortality rate (the fraction of individuals who die in the first period) corresponds to the area under the dashed red curve below the threshold. In the second period, this truncated distribution moves right again (if I is large relative to $d(1)$), and the population receives a new shock, generating mortality again among those with large negative shocks.

[4] The model can accommodate other distributions, but simulations with alternative assumptions (e.g., log normal errors) resulted in counterfactual mortality rates and a poorer overall fit.

[5] Our estimates for human populations find that $\alpha > 1$. The depreciation is therefore convex in age. Many empirical studies in gerontology have focused on the rate of aging, which corresponds to $\frac{\alpha H}{H} = \frac{-d\left(a\right)}{H}$ in our model. As in those studies and consistent with Dalgaard et al. (2019), we find that individuals with lower health levels age faster.

[6] See Gavrilov and Gavrilova (1991) and Weibull (1951) for attempts at biological microfoundations drawing on reliability theory from engineering.

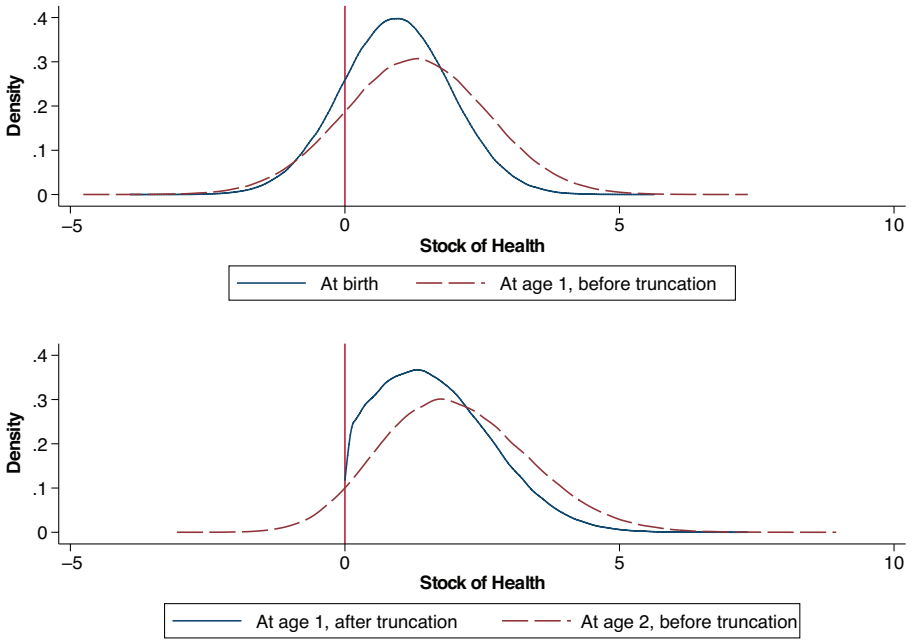

Fig. 2 Health and mortality in the first two years of life. Data are from simulations. The figure shows the evolution of the health distribution in the first two periods of life in a population where I exceeds the force of aging (δa^{a}) in the first two periods.

The stochastic term ε_a therefore plays a key role. In its absence, there would be no deaths in Period 2 or any subsequent period until the depreciation term becomes large enough to push the leftmost part of the distribution below the threshold.[7] Thereafter, mortality increases every period. Eventually everyone dies, which we prove more formally in online appendix C.

This basic model matches the stylized patterns described earlier. Figure 3 shows the evolution of the health distribution and the resulting mortality over the lifetime. Just like their empirical counterparts, cohorts in our model exhibit the following patterns: (1) the health distribution is roughly normal at most ages; (2) mean population health first increases and then falls with age; (3) the variance of health first increases and then falls with age; and (4) mortality first falls and then rises at a roughly log-linear rate after middle age. There is only one data feature we have not accounted for: the increase in mortality around adolescence.

Not all deaths have direct biological causes. Many deaths, such as accidents or homicides, strike individuals regardless of their health status. These extrinsic causes of death can be integrated into the model through the addition of an independent and identically distributed accident shock that is independent of the stock of health, H_a. Then, a constant fraction $\kappa \in [0,1]$ of the population is randomly killed every period.

[7] If I is less than aging, then one could generate positive mortality in the second period without a stochastic term. However, mortality would then rise from age 2 onward, which we do not observe in the data.

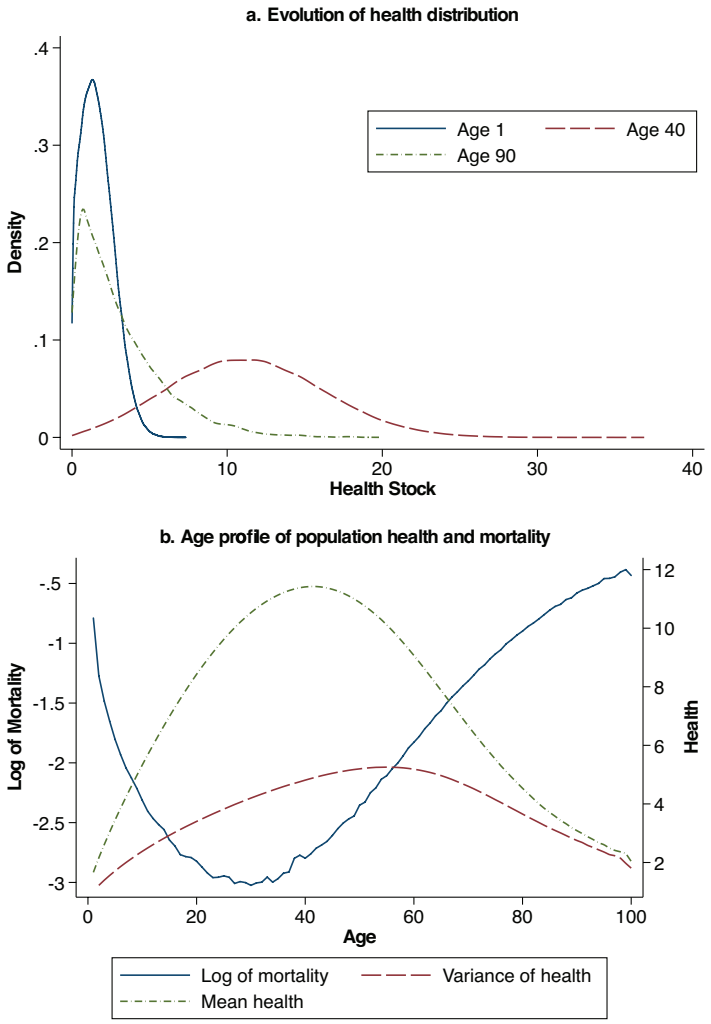

Fig. 3 Model behavior. Simulated data for a population of 500,000 individuals and without an adolescent hump. For this simulation, we use the following parameters: $I = 0.3575753$, $\delta = 0.0004789$, $\sigma = 0.8353752$, $\alpha = 1.7883$, and $\mu_0 = 0.925079$. Panel a shows the density of health for the population at ages 1, 40, and 90. Panel b plots average health, the variance of health, and mortality rates for the population over the lifetime, without external causes of death.

This random accident rate places a floor on the level of mortality that is constant across ages.[8]

Panel a of Figure 4 shows that adding a lifetime accident shock increases the mortality level at all ages but does not change its basic evolution. Adding mortality from

[8] If all health-related deaths were eliminated, this accident rate would uniquely determine the life expectancy of the population ($1 / \kappa$).

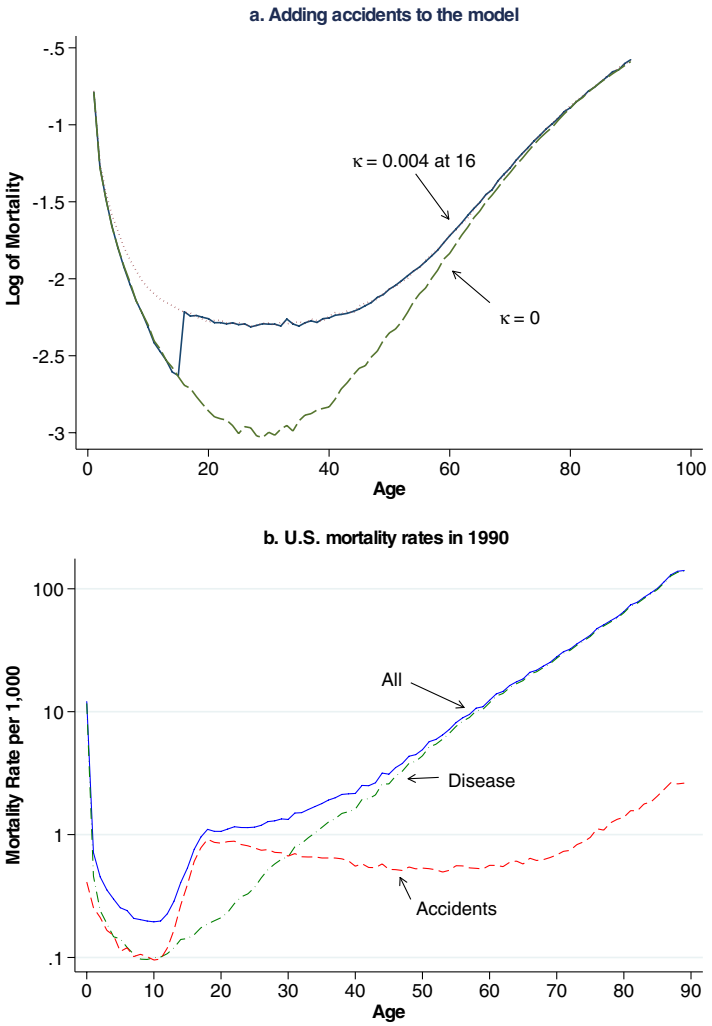

Fig. 4 Adding accidents to the baseline model. Panel a shows the evolution of mortality based on a simulation that uses the same baseline parameters as in Figure 3. The green dashed line shows the mortality curve without any accidents ($\kappa = 0$). The red dotted line shows the mortality curve of a population that experiences a $\kappa = 0.004\%$ chance of dying every period as a result of an accident, unrelated to health. The blue line shows the model that assumes the accident rate is 0 at birth but jumps to 0.004 in adolescence. Mortality rates are higher as a result of external deaths but more so among young adults because of competing risks: older individuals who experience an accident shock are also unhealthy and would die even in the absence of an accident shock. Panel b is reproduced from Schwandt and von Wachter (2020), who generously agreed to its use. The data come from *period* (not cohort) tables, so they are not directly comparable to ours. However, we use these data to demonstrate that the mortality rate from non-disease-related causes of death is well approximated by a step function that starts in adolescence. Mortality rates are shown in $\log_{10}$ scale.

accidents also does not affect the health distribution among the living because these deaths are random and do not depend on health status.

Contemporary data, however, show that the mortality rate from external causes of death is not constant throughout life. Instead, it is well approximated by a step function, with a major increase around adolescence (Figure 4, panel b). Among the young (ages 15–24), more than 80% of deaths are due to external deaths (Centers for Disease Control and Prevention 2019). On the basis of this evidence, we assume that κ starts at 0 but becomes positive in adolescence at an arbitrary age (a^*); we therefore add two more parameters to the model. For simplicity, we assume that the onset of adolescence is unaffected by health levels, and we take it to be exogenous.[9] Panel a of Figure 4 shows that adding this step function results in a profile of mortality that qualitatively matches the main features we observe.[10]

Explaining Mortality Patterns

We now assess whether the model can *quantitatively* match observed mortality patterns. To do so, we estimate the model parameters and assess the model's fit for both human and primate cohorts. We then compare our model to other demographic models.

Identification and Estimation

Identification

Two of the nine parameters of the full model cannot be identified. To see this, note that we can add or subtract any constant on both sides of the expression that determines the probability of dying, $D_a = \mathbb{I}\left(H_a \leq \underline{H}, D_{a-1} = 0\right)$, and leave the mortality rates at all ages unchanged. Thus, we must normalize either the level of initial health (μ) or the threshold ($\underline{H}$). Similarly, we can multiply each side of the equation by any positive constant and leave the probability of dying unchanged. Therefore, the scale of at least one variable must also be normalized. Without loss of generality, we set $\underline{H} = 0$ and $\sigma_H = 1$. After normalization, all the parameters are expressed in standard deviation units (except for α and κ, which are scale-free—they do not depend on the initial distribution). For example, we interpret μ_H as the distance from the threshold of the initial distribution, measured in standard deviations of the initial distribution.

The rescaled model characterizes the biological evolution of health and mortality of a cohort using seven (rescaled) parameters: one for the mean initial health

[9] This assumption could be relaxed. The onset of menarche, a proxy for adolescence in women, has declined from approximately age 16 to age 12 in the last two centuries. This development has been linked to nutritional changes and might be a function of health.

[10] The shapes in the two figures are not identical. However, the contemporary data are period data, not cohort data. In contemporary settings, the two profiles differ substantially. Unfortunately, no historical cohort mortality series by cause of death is available.

(μ_H), two governing the aging process (δ, α), two characterizing the effects of resources in the form of average investments (I) and the variance of these investments (σ^2), and two capturing the accident rate (κ) that starts in adolescence at age a^*. We do not estimate this last parameter. We assume that women's adolescence begins at the age at menarche, calculated as (−0.0175 × calendar year) +47.4. This equation was estimated by de La Rochebrochard (2000) using historical data from multiple sources. Adolescence is assumed to start one year later for men, as observed in contemporary settings. For chimpanzees, we draw on the literature to identify two alternative starting ages: 8 (Behringer et al. 2014) and 14 (Bronikowski et al. 2011).

Estimation

Despite the model's conceptual simplicity, the mortality rate at a given age cannot be expressed in closed form. We therefore estimate the parameters using the simulated method of moments: we generate data for a population and compare the resulting survival curve to the actual survival curve. The program iterates over the parameter space until the difference between the simulated and actual data is minimized. By matching the age-specific survival rates, we implicitly match life expectancy. See online appendix D for details.

Mortality Rates Over the Lifetime

We start by estimating the model for women born in 1816. The model closely matches their mortality rates at every age (Figure 5, panel a). The predicted life expectancy is 38 years and 102 days, and the actual life expectancy is 38 years and 91 days.

We estimate initial mean health to be 0.86, so many individuals are born at or below the threshold (Table A1). Absent any shocks or investment in the first period, infant mortality would have been roughly 15% (instead of 17%). Mortality falls dramatically after age 1 because of selection (many frail individuals have already died) and because investment is large relative to aging in the first period (I is estimated as 0.4, and δ is estimated as 0.0006).[11]

The estimated variance of resources is large (~1), so a few unlucky individuals still fall below the death threshold after age 2. Log mortality starts to increase steadily after age 45. This gradual increase occurs because δ is small (~0.0006), but the aging rate (α) is approximately 1.8, and the aging function δa^{α} thus increases more than linearly with age.

Accounting for external deaths is important: the fit of the model improves significantly, and the estimated parameters change (compare columns 1 and 2 of Table A1). The external mortality rate is 8.6 per thousand per year, lowering this cohort's life expectancy by approximately 7.6 years. This number is an upper-bound estimate of

[11] Health investments (I) are not technically needed to generate declining mortality in childhood.

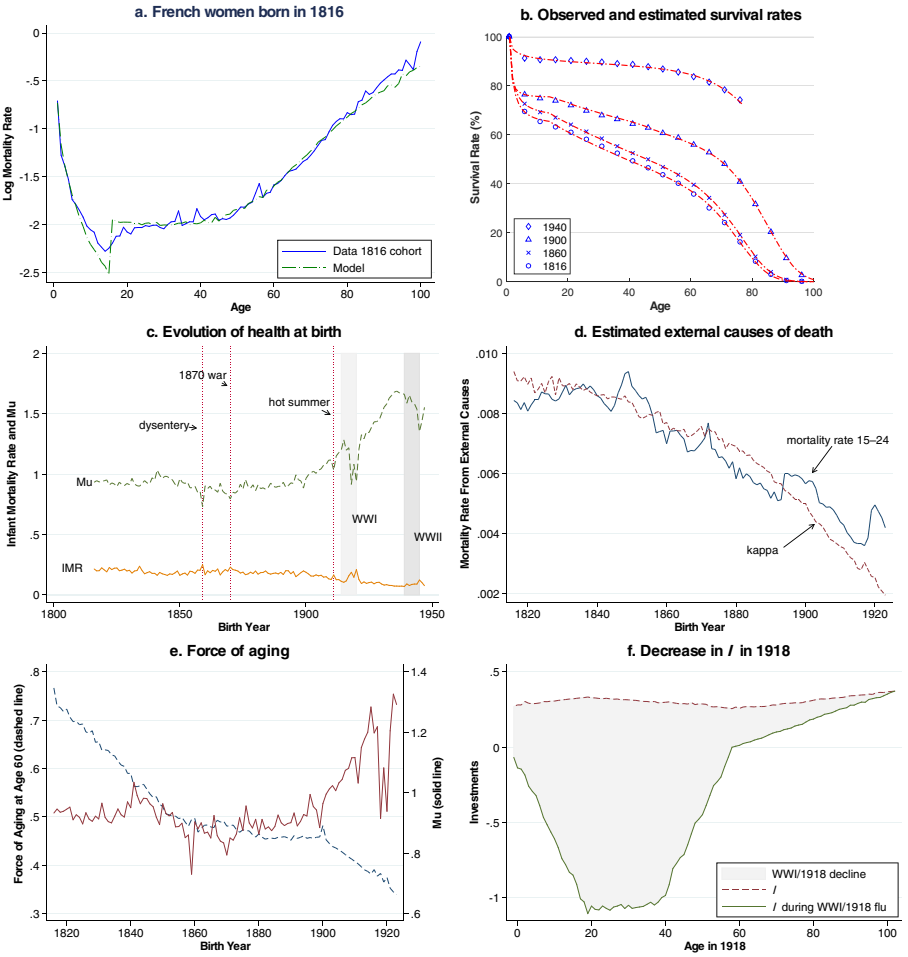

Fig. 5 Evolution of survival for French females born in 1816–1940. Panel a shows the observed mortality rates and the predicted rates for French women born in 1816. Panel b shows the observed (blue markers) and estimated (red dashes) survival curves for four cohorts of French women. Panel c shows the evolution of the infant mortality rate (IMR) and of health at birth (Mu, denoted by μ_0 in the model). Panel d shows the estimates of mortality from external causes (κ) alongside the average probability of dying across ages 15–24 (from cohort tables). Panel e shows the estimated function of aging at age 60, as $\delta(60)^{\alpha}$ and μ_0. Panel f shows the estimated effect of World War I and the 1918 flu pandemic on *I* as a function of age on the onset of the shock.

the effect of maternal mortality—the main cause of death for women in the nineteenth century—on life expectancy in the past.

These results are robust to several alternative estimation modifications, including using alternative weights, using an alternative objective function, and allowing for truncation at age 90. We also estimate models in which the onset of adolescence is normally distributed and estimated. These results (displayed in Table A2) show that the fit is not very sensitive to these alternatives.

Gender Differences

Figure A13 (panel a) shows the results for males born in 1816 (Table A1 reports the estimated parameters). Men born in 1816 had shorter lives than women. After accounting for the adolescent hump, which substantially improves the fit (column 4), we find that initial mean health is 18% lower for males than for females, consistent with males' greater frailty and higher infant mortality rates (Cullen et al. 2016; Goldin and Lleras-Muney 2019). Males receive slightly larger annual investments (about 10% greater) but experience greater variance in investments (5%). They also age faster in old age (although women age a bit faster during prime ages). The increase in deaths in adolescence is larger for men ($\kappa = 0.0097$), consistent with their greater involvement in accidents and violent deaths. However, because males have higher overall mortality rates, the elimination of accidental deaths would increase their life expectancy by approximately 7.6 years, similar to the predicted gains for women. Overall, the model fit is excellent for both genders, although the fit is better for females. Further, all parameters except for mean investments benefit women's survival.

Primates

Our model should describe mortality for nonhuman primates well: they live in relatively stable environments, experience no technological change, and have few optimization opportunities. Mortality patterns for nonhuman primates are also similar to those of humans. To estimate the model, we use the best available data on chimpanzees living in the wild, from Bronikowski et al. (2011). These populations, tracked in the wild from birth to death, have been used to compare mortality across various primate populations. We focus on chimpanzees because they are the closest primates (along with bonobos) to humans.

We obtain a very good fit, despite the smaller population size and therefore much noisier estimates (see panels b and c of Figure A13 and Table A3). Compared with human females, female chimps are born in better health, consistent with the observation that human infants are born frail relative to other species (for a discussion, see Rosenberg and Trevathan 1995). They have a lower rate of accidental deaths, consistent with maternal mortality being a uniquely important problem among humans (Rosenberg 1992).[12] Other parameters, however, favor longevity among human females. In chimps, the estimated annual investment (I) is approximately 20% smaller, and the variance of I is 10% larger than among humans. Most notably, δ is much larger for chimps than for humans (0.06 vs. 0.0006), resulting in much faster aging. As for humans, female chimps live longer than males, partly because males have larger external causes of death than females. Males also have larger annual investments, larger variance in resources, and a larger aging parameter (α) than females. Unlike humans, though, male chimps have larger estimated initial health than female chimps.

[12] Rosenberg (1992:100) stated that "most primates experience parturition as a simpler, shorter, and very likely less painful process" than humans. Our estimates do not imply that external causes of death are unimportant among primates; neither model estimates a baseline accident rate throughout.

The Rectangularization of Survival and the Sources of Life Expectancy Increases

Remarkably, the model is able to track the evolution of the mortality profiles for all the cohorts born since 1816. This evolution is characterized by a rectangularization of the survival curves. Panel b of Figure 5 illustrates this using the survival curves of French women born in 1816, 1860, 1900, and 1940. Survival to age 1 has increased dramatically. The next section of the survival curve, roughly from ages 1 to 60, flattened considerably. In addition, a steep downward slope emerged among the oldest. As a result, more than 70% of those born in 1940 lived past age 70, compared with less than 30% of those in the 1816 cohort. The model captures this rectangularization accurately: the observed (blue markers) and estimated (red dashes) survival curves are very similar for all cohorts. The results are similar for men (Table A4).

What are the sources of increases in longevity according to our estimates? Health at birth (μ_H) was stagnant for most of the nineteenth century and then increased dramatically around 1900 (Figure 5, panel c). But μ_H dropped for cohorts born during epidemics (1858, 1870, and 1918), extreme weather events (e.g., the extremely hot summer of 1911), and wars (1870, World War I, and World War II). These patterns mirror the evolution of infant mortality. It fell after 1900 because improvements in water, sanitation, and the dissemination of best infant-feeding practices (breastfeeding, milk pasteurization, and water boiling) reduced infectious disease mortality (Corsini and Viazzo 1993; Kesztenbaum and Rosenthal 2017; Preston and van de Walle 1978); it increased during wars, pandemics, and hot summers.

We also observe a secular decline in external causes of death (Figure 5, panel d), consistent with the elimination of maternal mortality—a major cause of death among prime-aged women in the past (Loudon 1988)—and with the decline in violent deaths, as documented by Pinker (2011). This decline in external causes of death tracks the decline in the probability of dying among 15- to 24-year-olds (solid blue line). The level of κ is similar to the level of mortality among the young, as predicted by the model and consistent with contemporary data (Figure 4, panel a).

Finally, we observe a substantial decrease in the force of aging before 1840 and after 1900, the causes of which are unclear (we plot it at age 60: $\delta(60)^{\alpha}$ in panel e of Figure 5). Since food consumption and heights rose after 1900, this suggests that nutrition is a possible determinant of the aging function (Fogel 1994). Interestingly, the aging function declines around 1900 at the same time that μ_H rises and infant mortality declines. These findings are consistent with Finch and Crimmins's (2004:1736) observation of "strong associations between early-age mortality and subsequent mortality in the same cohorts," which they attribute to the decline in exposure to infectious diseases, which lead to inflammation.

By contrast, health resources (I) did not change much in the nineteenth century (they declined a bit and rose again), consistent with the debate on the questionable benefits of the Industrial Revolution on health and living standards. However, events such as the World War I/1918 flu pandemic substantially reduce these resources while they are taking place. Panel f of Figure 5 shows a substantial temporary decline in I at this time. This decline was greatest among individuals aged 20–40, consistent

with the observation that the 1918 pandemic had its largest effects among prime-aged adults (Murray et al. 2006).

Finally, the variance of health resources declined steadily. The explanation for this decline is unclear, although it is possible that food availability became less variable (Figure A14).[13] These last two parameters (I, σ) are the most difficult to assess against external data because they represent the distribution of health resources over a lifetime.[14]

Figure A15 shows the performance of the model for cohorts born in 1816–1923 (the last cohort with complete data up to age 90). The fit is excellent throughout the nineteenth century, but it deteriorates after 1900 for a few reasons. First, two events in the early twentieth century are likely to severely affect these cohorts: the World War I/1918 flu pandemic and World War II. Later, we discuss how we estimated these events, but they are difficult to model. The data during these episodes are also of lower quality because changes in territory, for example, make the computations of death rates challenging. Finally, we assume that no intertemporal optimization is occurring. The rise of social insurance programs throughout the twentieth century suggests that this assumption is likely violated for recent cohorts. We discuss optimization and its effects at the end of the paper.

Comparison With Alternative Demographic Models

We compare the fit of our model to the classic Gompertz (1825) model, the popular Heligman and Pollard (1980) model, a subsequent model developed by Carriere (1992), and the vitality model by Sharrow and Anderson (2016) (see online appendix B). We estimate these four models and ours for men and women born in 1816 and 1921. We compute three measures of fit: the RMSE (root-mean-square error) of the survival curve, the RMSE of the log mortality rates, and the predicted life expectancy.

The results (displayed in Table A6) show that the Heligman and Pollard model provides the best fit for all cohorts, but our model is very close despite using fewer parameters. Further, our model performs better than more recent models, and unlike the Heligman and Pollard model, we can achieve other aims of recent demographic models.

Understanding Mortality Dynamics

In this section, we conduct qualitative exercises to demonstrate that the model can rationalize the effects on mortality of temporary and permanent shocks documented in the literature as resulting from simple shocks to the model parameters.

[13] It might be difficult for the model to separately identify the effects of I from the effects of its variance because the mortality data are informative only about the left tail of the health distribution.

[14] Future research could improve this estimation by imposing that overlapping cohorts share the same resources. However, this is not a trivial exercise: it would require making additional assumptions and altering the estimation procedure to simultaneously estimate several hundreds of parameters.

SES Mortality Gradient

A substantial literature documents health and mortality gradients—large and persistent differences across individuals with different levels of SES, such as education or income (Cutler et al. 2012).

How can the model rationalize such gradients? Suppose that we extend our model so that higher income leads to higher I throughout life—that there exists a function $I=I(Y, E)$ with $\frac{\partial I}{\partial Y} > 0$ and $\frac{\partial I}{\partial E} > 0$. We illustrate the effect of lowering Y by simulating the effect of lowering I by 50% for the 1816 French female cohort (Figure 6). This simulation results in higher and flatter log mortality curves for the lower income population compared to the initial richer population (panel a). Moreover, the curves for the high- and low-income populations converge in old age (panel b), as Chetty et al. (2016) documented. This occurs because, although the frailest individuals die in the first period when Y falls (potentially lowering mortality), Y shifts the distribution of health left in all subsequent periods, increasing mortality thereafter.

An examination of the profile over the lifetime (Figure 6, panel c) reveals that the narrowing of the mortality gap occurs in the model *only after a certain age*. In log (percentage) terms, the mortality gap initially grows with age but eventually falls. In *levels*, however, SES gaps in mortality rates are U-shaped (instead of hump-shaped) with age, as Kaestner et al. (2020) illustrated (for education) and as the cumulative advantage hypothesis predicts (Lynch 2003; Ross and Wu 1995). The reason the patterns differ in levels and logs is that the log specification captures percentage changes, dividing the SES gaps (in levels) by the baseline mortality, which is also U-shaped.

Health

Lower income (or education) and thus lower I also lower average health at all ages. However, the effect increases with age and then declines in both levels and percentage terms because mortality starts rising (Figure 6, panel d). These predictions match the evidence from Case et al. (2002), Currie and Stabile (2003), and House et al. (2005), who showed that health gaps between those born in low-income families and those born in high-income families grow with age but decline after 65.

Resource Scarcity or Accelerated Aging?

Higher SES is associated with more frequent physical exercise, lower exposure to pollution, and lower stress, which may affect the rate of depreciation (instead of the level of resources).[15] In the model, an increase in the aging parameters (δ or α) and a decrease in I generate similar changes in the health and mortality

[15] For example, Liu et al. (2019) found that education and race are associated with lower methylation rates, a biomarker for aging.

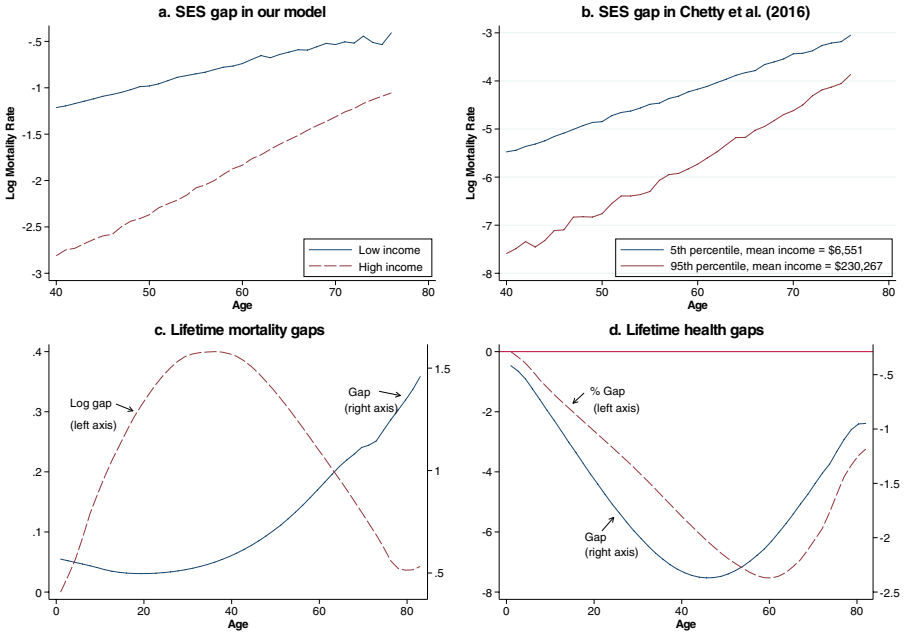

Fig. 6 Generating SES gradients in health and mortality. Panel a shows the predicted mortality rate for the 1816 cohort (using the parameters from Table A1 but setting the accident rate at 0 throughout for simplicity) and the counterfactual mortality that results from a 95% decline in I for this population. The baseline 1816 cohort is labeled "High income," and the counterfactual population is labeled "Low income." Panel b reproduces the results from Chetty et al. (2016) and shows the mortality rates of high- and low-income populations in the United States. Panel c shows the simulated effects of decreasing the baseline level of I (our proxy for SES) by 50% on mortality in levels and percentages. We plot the gap between the baseline and the affected population. This gap is computed as $MR(low\ SES) - MR(high\ SES)$. Panel d shows the effects of increasing the baseline level of I by 50% on health. This gap is computed as $H(low\ SES) - H(high\ SES)$. The baseline parameters are the same as in Figure 3.

profiles among the old, as shown in Figure A16. However, higher aging rates do not result in any visible health or mortality gaps among children, whereas higher I does. Therefore, the evidence from Case et al. (2002), Currie and Stabile (2003), and House et al. (2005), interpreted through the lens of the model, suggests that changing family income is equivalent to changing I, although both processes could be at play.

It would be ideal to reestimate our model using cohort data by education or income, but data tracking *cohorts* from birth to death by family income or education levels are not available. Our simulations show only that the model can rationalize the observed patterns in the data.[16]

[16] One could reestimate the model for the aggregate data as a mixture of the evolution of two populations with different SES levels. In the absence of data by SES, this would only add more parameters to the model.

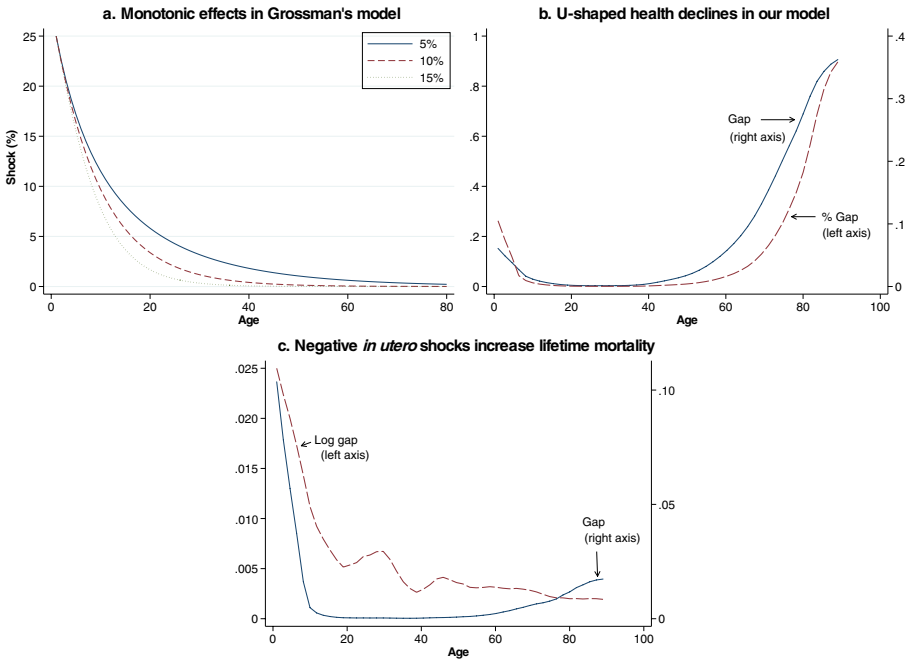

Fig. 7 The effects of negative *in utero* shocks. Panel a reproduces and extends a figure in Almond and Currie (2011: figure 1) and shows the decline in the health stock due to a 25% shock *in utero* that is predicted by the standard Grossman model. We simulate the evolution of health for two populations using Grossman's equation for the evolution of health (also Almond and Currie 2011: equation 1), which states that $H_t = (1-\delta)H_t + I_t$. We set $\mu_0 = 10$ for one population and $\mu_0 = 7.5$ for the shocked population; we set $I = 1$ for both populations. The figure displays the differences in H by age, expressed in percentages relative to the baseline population. This effect is initially large but fades over time and will be close to 0 among adults older than 30; the extent of this fading depends on the depreciation rate, which we set at 5%, 10%, and 15%. Panel b shows the simulated effects of a 50% decline in health *in utero* for the 1816 French population in our model (with the accident rate set at 0 throughout for simplicity). The figure plots the decreases in health in levels or percentages. In contrast to the Grossman model, our model predicts a U-shaped pattern of effects: high in childhood, low in middle age, and increasing among the old. Panel c shows the effects on mortality of a 50% decline in health *in utero* in levels and percentages. The figure shows that mortality increases as a result, and the age pattern of the effects varies depending on whether we express them in levels or logs. The baseline parameters used in panels b and c are the same as in Figure 3.

Nonmonotonic Effects of *In Utero* Shocks

Detrimental events *in utero* (e.g., famine, war, recession) result in large and persistent health declines that are visible in infancy and old age (Barker et al. 1993) and in elevated mortality among the survivors. Empirically, these effects are initially large and then appear to fade, only to reappear later in life (for a comprehensive review, see Almond et al. 2018). As Almond and Currie (2011) noted, though, the Grossman model predicts immediate declines in health that are hardly visible by adulthood (Figure 7, panel a).

What does our model predict? Suppose that we allow for the initial mean of the distribution, μ_H, to be affected by outside forces F ($\mu_H = \mu_H(F)$, $\mu_H' > 0$).

We use the 1816 parameters to simulate the effect of exogenously lowering F, and thus μ_H, on the survivors' subsequent health and mortality (Figure 7, panel b). Lowering initial health, μ_H, by 50% lowers health among the survivors at all ages—both in levels and in percentages—with a U-shaped pattern in age, exactly as the literature documents. For example, Schiman et al. (2017) found that the effects of experiencing World War II *in utero* and early childhood on health, disability, and employment are not visible for young adults but grow with age, as predicted here. The reason this happens in our model but not in Grossman's is that depreciation in our model is not multiplicative in the stock. Like ours, Dalgaard et al.'s (2019) model of health deficits also predicts that *in utero* shocks will result in health gaps that increase with age among adults. However, our model predicts a U-shaped pattern of effects rather than a monotonically increasing effect. This U-shape results from our having an early childhood period in which investments move the distribution of health up.[17] These results also suggest that it is impossible to identify the effects of *in utero* shocks with health data for adolescents or young adults only.

Mortality

Mortality at all ages also increases when initial conditions worsen (Figure 7, panel c). Again, the age patterns depend on the metrics used. When measured in levels, the effects are U-shaped. The intuition for this U-shaped pattern is simple. Among adolescents and young adults, the average health level is high, and very few individuals are close to the threshold, so shifting the distribution of health has very little impact on mortality. But shifts in the distribution will result in higher death rates when the distribution gets closer to the threshold at older ages. When expressed in percentage terms, however, the predicted effects of negative *in utero* shocks on mortality fall with age (although this pattern is not necessarily monotonic: in middle age, when mortality levels are low, the effects can rise and fall because of the small number of deaths).

An important implication of our simulations for the empirical literature is that the predictions for the dynamic effects of shocks on mortality are sensitive to the functional form one chooses for studying its effects.

Scarring Effects of Wars

Wars have long-lasting detrimental health effects among survivors. Such scarring effects have been documented in at least 13 European countries after World War II. Compared with less-exposed survivors, individuals who were more exposed to the war experienced worse economic and health outcomes that persisted several decades later (e.g., Havari and Peracchi 2017; Kesternich et al. 2014). Similarly, Wilson et al.

[17] With data on health over the lifetime, these different predictions could be verified.

(2014) showed the persistence of higher mortality rates among New Zealand military personnel who served during the war than among those who did not.

Suppose we model war episodes as reducing health resources (I).[18] Panel a of Figure 8 shows the mortality curves obtained from estimating the model for men born in 1896 with two shocks: a four-year decline in I at age 18 (corresponding to the combined effects of World War I and the 1918 flu pandemic) and a six-year decline in I at age 43 (corresponding to the effects of World War II). This simple characterization of the wars delivers a mortality curve (red dotted line) that is remarkably close to the data (blue line). When the war shocks are eliminated, mortality falls during the war and at all subsequent ages (red dashed line). Thus, the model predicts the scarring effects that other authors have documented: the mortality rates for the affected cohort are persistently higher than those for unaffected cohorts, both during the war and after. We estimate that World War I lowered life expectancy by approximately 16 years for this cohort, and that World War II lowered it by another 2 years.[19]

Harvesting Effects

Extreme weather or pollution events appear to displace the distribution of deaths in the short term, creating a sudden increase in the number of deaths followed by abnormally low mortality. In demography, this phenomenon is known as "harvesting" and has been, for instance, documented in France during the 2003 heat wave (Toulemon and Barbieri 2008).[20]

How can the model rationalize this pattern? Suppose that the death threshold is a function of the environment ($\underline{H} = \underline{H}\left(E\right)$, $\underline{H}' > 0$). Panel b of Figure A17 shows the simulated effect of a temporary increase in the threshold at ages 60 and 61 on the mortality of the 1816 cohort. This temporary increase results in very high initial mortality that starts dropping before the shock ends because the frailest individuals have already died. Once the weather disruption ends and the threshold is restored to its original (lower) level, mortality falls even more because there are very few individuals close to the new lower threshold. Mortality remains below its counterfactual level until the aging process lowers health stocks again. Thus, a death threshold change generates harvesting, and it does so by killing the least healthy individuals in the cohort. A key characteristic of a threshold change is that it does not affect the health of the living.[21]

[18] This assumption is consistent with historical data for World War II. GDP declined during the war, and the Germans appropriated 20% to 55% of it during the occupation (Occhino et al. 2007). Food rationing began in 1940. We can assume that the war is a different type of shock, but we do not obtain better fits with these alternatives.

[19] The fit for this cohort can be improved if we allow every year of a war to have its own effect instead of imposing an equal annual shock during wars (Table A5).

[20] See Schwartz (2000) and Zeger et al. (1999) for the effects of pollution; see Deschênes and Moretti (2009) and Deschênes and Greenstone (2011) for the effects of extreme temperatures.

[21] Weather shocks may affect survivors' health. See Deschênes and Moretti (2009) and Deschênes and Greenstone (2011) for a discussion.

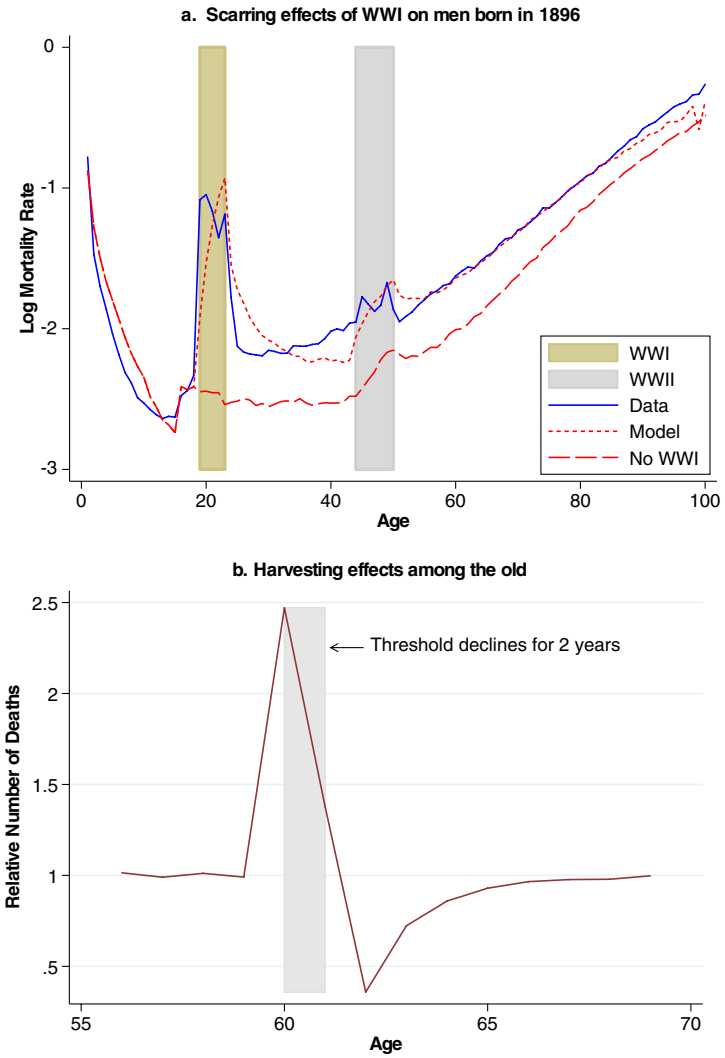

Fig. 8 Scarring and harvesting effects. Panel a shows the scarring effect of World War I on mortality rates for men born in France in 1896 who turned 18 when the war started in 1914 and who would have served in the military. The solid blue line shows the observed mortality rates for this cohort. The dotted red line shows the predicted mortality rates that result from estimating the model and including an additional parameter for World War I and another for World War II. We allow for I to differ during each war. The counterfactual curve (dashed red line) shows what the mortality curve would look like in the absence of World War I by predicting what the rates would have been in the absence of a decline in I during that war. Panel b shows the simulated effects of a temporary increase in the threshold (from 0 to 0.8) at ages 60 and 61 in the 1816 French cohort (setting the accident rate to 0 for simplicity). The y-axis plots the relative number of deaths in the affected population divided by the number of deaths in the unaffected population. The figure shows that deaths are shifted earlier. This displacement is estimated to result in approximately 8,000 excess deaths during the shock and fewer deaths in the subsequent two years.

Heat waves and other forms of bad weather also generate excess mortality among children (Figure A17, panel b), but the displacement effect is substantially more spread out. In other words, the children who die as a result of the bad weather would not die immediately after the bad weather ends; they would live substantially longer lives. (Among children, investment levels are high relative to depreciation, and mortality is falling, whereas depreciation is large and mortality increases among the elderly.)

The Effects of Temporary and Permanent Shocks

The previous two sections illustrate the effects of temporary changes in I or $\underline{H}$, but they do not compare their effects on the same scale because we aimed to reproduce published results. Figure A18 shows how log mortality rates respond to all types of temporary shocks. Each shock leaves a unique imprint on mortality rates. Temporary investment and depreciation decreases have similar scarring effects: mortality rises when the shock starts and then starts falling after the shock ends, but it does not return to its counterfactual level. On the other hand, only changes in the threshold generate harvesting. Only variance changes result in a crossover of mortality rates at old ages, and only accident increases leave mortality rates unchanged once the shock ends. Figure A19 further reveals that the pattern of these responses over time is not the same when viewed in logs or levels. For comparison, Figure A20 shows the effects of permanent shocks on all parameters in levels and logs.

Optimization

So far, we considered a population that receives constant investments over the lifetime. In online appendix E, we estimate the optimal investment profile that a social planner would choose to maximize life expectancy. We assume that the planner has a fixed lifetime budget and the ability to borrow and save costlessly, so the planner can invest different levels of I at different ages so long as they add up to the total budget.[22] We find that the optimal strategy for maximizing life expectancy is to redistribute resources from prime-aged adults to children and the elderly. Doing so would increase the life expectancy of French women born in 1816 by three years—a considerable but smaller gain than observed in the data. After optimization, the resulting survival curves are flatter in adulthood and steeper at old ages, suggesting that the rectangularization of survival is partly due to the emergence of optimization.

Conclusion

We propose a parsimonious production function to study the evolution of health and mortality over the life course of a population born with heterogeneous health

[22] This is a standard assumption (e.g., see Murphy and Topel 2006).

endowments. Despite its simplicity, this model tracks the evolution of the mortality profile of human cohorts born in 1816–1940, as well as nonhuman primates. Further, the model can explain many important mortality patterns documented in the literature, including the rectangularization of survival curves and SES gradients in health. We also show how to use the model to understand the dynamic treatment effects of *in utero* shocks and other temporary events, such as wars.

The model's parsimony relies on transparent but strong parametric assumptions. In particular, we assume that the environment is stable and exogenously provides a constant level of resources. These assumptions are reasonable for primates or early human populations but not for contemporary populations with access to saving technologies, growing GDP, and medical innovations. We explore how to incorporate changes in the environment into the model, but further progress could be made by using data on environmental changes as inputs and by making restrictions across cohorts. We also assume that health shocks are independent and identically distributed, and normally distributed. Alternative assumptions for this distribution of annual shocks could be further investigated. The model can also be expanded to consider the role of behavior and policy. Our preliminary analysis suggests that in the absence of financial frictions, optimal health expenditures are U-shaped over the lifetime in this model. With additional data, the implications of optimizing behavior could be explored further. We leave these explorations to future research. ■

Acknowledgments The views expressed in this article are those of the authors and do not necessarily represent the views of the International Monetary Fund, its Executive Board, or IMF management. We are very grateful to David Atkin, Andy Atkeson, David Cutler, Jeff Ely, Price Fishback, Titus Galama, Patrick Heuveline, Bo Honoré, Wei Huang, and Jonanthan Skinner for their advice, and to seminar participants at Stanford University, University of British Columbia, University of Connecticut, University of Southern California, and University of California Los Angeles, as well as the NBER Cohort meetings. We are also grateful to Hualei Shang, Sungwoo Cho, and Wan Zhang for their outstanding research assistance. This work used computational and storage services associated with the Shared Hoffman2 Cluster provided by the UCLA Institute for Digital Research and Education's Research Technology Group. This project was supported by the California Center for Population Research at UCLA, which receives core support (P2C-HD041022) from the Eunice Kennedy Shriver National Institute of Child Health and Human Development. All errors are our own.

References

Allen, S. V., & Hopkins, W. G. (2015). Age of peak competitive performance of elite athletes: A systematic review. *Sports Medicine, 45,* 1431–1441.

Almond, D., & Currie, J. (2011). Killing me softly: The fetal origins hypothesis. *Journal of Economic Perspectives, 25*(3), 153–172.

Almond, D., Currie, J., & Duque, V. (2018). Childhood circumstances and adult outcomes: Act II. *Journal of Economic Literature, 56,* 1360–1446.

Armitage, P., & Doll, R. (1954). The age distribution of cancer and a multi-stage theory of carcinogenesis. *British Journal of Cancer, 8,* 1–12.

Barker, D. J. P., Godfrey, K. M., Gluckman, P. D., Harding, J. E., Owens, J. A., & Robinson, J. S. (1993). Fetal nutrition and cardiovascular disease in adult life. *Lancet, 341,* 938–941.

Baxter-Jones, A. D. G., Faulkner, R. A., Forwood, M. R., Mirwald, R. L., & Bailey, D. A. (2011). Bone mineral accrual from 8 to 30 years of age: An estimation of peak bone mass. *Journal of Bone and Mineral Research, 26,* 1729–1739.

Behringer, V., Deschner, T., Deimel, C., Stevens, J. M. G., & Hohmann, G. (2014). Age-related changes in urinary testosterone levels suggest differences in puberty onset and divergent life history strategies in bonobos and chimpanzees. *Hormones and Behavior, 66,* 525–533.

Benyamini, Y., & Idler, E. L. (1999). Community studies reporting association between self-rated health and mortality: Additional studies, 1995 to 1998. *Research on Aging, 21,* 392–401.

Bronikowski, A. M., Altmann, J., Brockman, D. K., Cords, M., Fedigan, L. M., Pusey, A., . . . Alberts, S. C. (2011). Aging in the natural world: Comparative data reveal similar mortality patterns across primates. *Science, 331,* 1325–1328.

Carnes, B. A., Olshansky, S. J., & Grahn, D. (1996). Continuing the search for a law of mortality. *Population and Development Review, 22,* 231–264.

Carriere, J. F. (1992). Parametric models for life tables. *Transactions of the Society of Actuaries, 44,* 77–99.

Case, A., & Deaton, A. S. (2005). Broken down by work and sex: How our health declines. In D. A. Wise (Ed.), *Analyses in the economics of aging* (pp. 185–212). Chicago, IL: University of Chicago Press.

Case, A., Lubotsky, D., & Paxson, C. (2002). Economic status and health in childhood: The origins of the gradient. *American Economic Review, 92,* 1308–1334.

Centers for Disease Control and Prevention. (2019). Percentage of deaths from external causes, by age group—United States, 2017. *Morbidity and Mortality Weekly Report, 68,* 710.

Chetty, R., Stepner, M., Abraham, S., Lin, S., Scuderi, B., Turner, N., . . . Cutler, D. (2016). The association between income and life expectancy in the United States, 2001–2014. *JAMA, 315,* 1750–1766.

Corsini, C. A., & Viazzo, P. P. (Eds.). (1993). *The decline of infant mortality in Europe, 1800–1950: Four national case studies* (UNICEF report). Florence, Italy: United Nations Children's Fund, International Child Development Centre; Florence, Italy: Istituto degli Innocenti.

Cullen, M. R., Baiocchi, M., Eggleston, K., Loftus, P., & Fuchs, V. (2016). The weaker sex? Vulnerable men and women's resilience to socio-economic disadvantage. *SSM–Population Health, 2,* 512–524.

Currie, J., & Stabile, M. (2003). Socioeconomic status and child health: Why is the relationship stronger for older children? *American Economic Review, 93,* 1813–1823.

Cutler, D. M., Lleras-Muney, A., & Vogl, T. (2012). Socioeconomic status and health: Dimensions and mechanisms. In S. Glied & P. C. Smith (Eds.), *The Oxford handbook of health economics* (pp. 124–163). Oxford University Press.

Dalgaard, C.-J., Hansen, C. W., & Strulik, H. (2019). *Accounting for fetal origins: Health capital vs. health deficits* (CEGE Discussion Papers, No. 385). Göttingen, Germany: Center for European, Governance and Economic Development Research.

Dalgaard, C.-J., Hansen, C. W., & Strulik, H. (2021). Fetal origins? A life cycle model of health and aging from conception to death. *Health Economics, 30,* 1276–1290.

Dalgaard, C.-J., & Strulik, H. (2014). Optimal aging and death: Understanding the Preston curve. *Journal of the European Economic Association, 12,* 672–701.

Deaton, A. S., & Paxson, C. H. (1998). Aging and inequality in income and health. *American Economic Review: Papers & Proceedings, 88,* 248–253.

de La Rochebrochard, E. (2000). Age at puberty of girls and boys in France: Measurements from a survey on adolescent sexuality. *Population: An English Selection, 12,* 51–79.

Deschênes, O., & Greenstone, M. (2011). Climate change, mortality, and adaptation: Evidence from annual fluctuations in weather in the U.S. *American Economic Journal: Applied Economics, 3*(4), 152–185.

Deschênes, O., & Moretti, E. (2009). Extreme weather events, mortality, and migration, *Review of Economics and Statistics, 91,* 659–681.

Finch, C. E., & Crimmins, E. M. (2004). Inflammatory exposure and historical changes in human lifespans. *Science, 305,* 1736–1739.

Fogel, R. W. (1994). Economic growth, population theory, and physiology: The bearing of long-term processes on the making of economic policy. *American Economic Review, 84,* 369–395.

Galama, T. J., & van Kippersluis, H. (2019). A theory of socio-economic disparities in health over the life cycle. *Economic Journal, 129,* 338–374.

Ganna, A., & Ingelsson, E. (2015). 5 year mortality predictors in 498 103 UK Biobank participants: A prospective population-based study. *Lancet*, *386*, 533-540.

Gavrilov, L. A., & Gavrilova, N. S. (1991). *The biology of life span: A quantitative approach.* New York, NY: Harwood Academic Publishers.

Goldin, C., & Lleras-Muney, A. (2019). XX > XY?: The changing female advantage in life expectancy. *Journal of Health Economics, 67,* 102224. https://doi.org/10.1016/j.jhealeco.2019.102224

Gompertz, B. (1825). On the nature of the function expressive of the law of human mortality, and on a new mode of determining the value of life contingencies. *Philosophical Transactions of the Royal Society of London, 115,* 513–583.

Grossman, M. (1972). On the concept of health capital and the demand for health. *Journal of Political Economy, 80,* 223–255.

Halliday, M. H., Garcia, A. N., Amorim, A. B., Machado, G. C., Hayden, J. A., Pappas, E., . . . Hancock, M. J. (2019). Treatment effect sizes of mechanical diagnosis and therapy for pain and disability in patients with low back pain: A systematic review. *Journal of Orthopaedic & Sports Physical Therapy, 49,* 219–229.

Halliday, T. (2011). Health inequality over the life-cycle. *B.E. Journal of Economic Analysis & Policy, 11*(3). https://doi.org/10.2202/1935-1682.2758

Halliday, T., Mazumder, B., & Wong, A. (2018). *Intergenerational health mobility in the U.S.* (IZA Discussion Paper, No. 11304). Bonn, Germany: Institute of Labor Economics.

Havari, E., & Peracchi, F. (2017). Growing up in wartime: Evidence from the era of two world wars. *Economics & Human Biology, 25,* 9–32.

Heligman, L., & Pollard, J. H. (1980). The age pattern of mortality. *Journal of the Institute of Actuaries, 107,* 49–80.

House, J. S., Lantz, P. M., & Herd, P. (2005). Continuity and change in the social stratification of aging and health over the life course: Evidence from a nationally representative longitudinal study from 1986 to 2001/2002 (Americans' Changing Lives Study). *Journals of Gerontology, Series B: Psychological Sciences and Social Sciences, 60*(Special issue 2), S15–S26.

Human Mortality Database. (2017). Berkeley (USA): University of California, Berkeley; Rostock, Germany: Max Planck Institute for Demographic Research. Available from www.mortality.org

Idler, E. L., & Benyamini, Y. (1997). Self-rated health and mortality: A review of twenty-seven community studies. *Journal of Health and Social Behavior, 38,* 21–37.

Kaestner, R., Schiman, C., & Ward, J. (2020). Education and health over the life cycle. *Economics of Education Review, 76,* 101982. https://doi.org/10.1016/j.econedurev.2020.101982

Kesternich, I., Siflinger, B., Smith, J. P., & Winter, J. K. (2014). The effects of World War II on economic and health outcomes across Europe. *Review of Economics and Statistics, 96,* 103–118.

Kesztenbaum, L., & Rosenthal, J.-L. (2017). Sewers? Diffusion and the decline of mortality: The case of Paris, 1880–1914. *Journal of Urban Economics, 98,* 174–186.

Li, T., & Anderson, J. (2013). Shaping human mortality patterns through intrinsic and extrinsic vitality processes. *Demographic Research, 28,* 341–372. https://doi.org/10.4054/DemRes.2013.28.12

Liu, Z., Chen, B. H., Assimes, T. L., Ferrucci, L., Horvath, S., & Levine, M. E. (2019). The role of epigenetic aging in education and racial/ethnic mortality disparities among older U.S. women. *Psychoneuroendocrinology, 104,* 18–24.

Loudon, I. (1988). Maternal mortality: 1880–1950. Some regional and international comparisons. *Social History of Medicine, 1,* 183–228.

Lynch, S. M. (2003). Cohort and life-course patterns in the relationship between education and health: A hierarchical approach. *Demography, 40,* 309–331.

McGee, D. L., Liao, Y., Cao, G., & Cooper, R. S. (1999). Self-reported health status and mortality in a multiethnic U.S. cohort. *American Journal of Epidemiology, 149,* 41–46.

Metter, E. J., Lynch, N., Conwit, R., Lindle, R., Tobin, J., & Hurley, B. (1999). Muscle quality and age: Cross-sectional and longitudinal comparisons. *Journals of Gerontology, Series A: Biomedical Sciences and Medical Sciences, 54,* B207–B218.

Murphy, K. M., & Topel, R. H. (2006). The value of health and longevity. *Journal of Political Economy, 114,* 871–904.

Murray, C. J. L., Lopez, A. D., Chin, B., Feehan, D., & Hill, K. H. (2006). Estimation of potential global pandemic influenza mortality on the basis of vital registry data from the 1918–20 pandemic: A quantitative analysis. *Lancet, 368,* 2211–2218.

Occhino, F., Oosterlinck, K., & White, E. N. (2007). How occupied France financed its own exploitation in World War II. *American Economic Review: Papers & Proceedings, 97,* 295–299.

Olshansky, S. J., Hayflick, L., & Carnes, B. A. (2002). No truth to the fountain of youth. *Scientific American, 286*(6), 92–95.

Palloni, A., & Beltrán-Sánchez, H. (2017). Discrete Barker frailty and warped mortality dynamics at older ages. *Demography, 54,* 655–671.

Pinker, S. (2011). *The better angels of our nature: Why violence has declined*. New York, NY: Viking Penguin.

Pompei, F., & Wilson, R. (2002). A quantitative model of cellular senescence influence on cancer and longevity. *Toxicology and Industrial Health, 18,* 365–376.

Preston, S., Heuveline, P., & Guillot, M. (2000). *Demography: Measuring and modeling population processes.* Oxford, UK: Blackwell Publishers.

Preston, S. H., & van de Walle, E. (1978). Urban French mortality in the nineteenth century. *Population Studies, 32,* 275–297.

Rosenberg, K., & Trevathan, W. (1995). Bipedalism and human birth: The obstetrical dilemma revisited. *Evolutionary Anthropology: Issues, News, and Reviews, 4,* 161–168.

Rosenberg, K. R. (1992). The evolution of modern human childbirth. *American Journal of Physical Anthropology, 35*(S15), 89–124.

Ross, C. E., & Wu, C.-l. (1995). The links between education and health. *American Sociological Review, 60,* 719–745.

Schiman, J. C., Kaestner, R., & Lo Sasso, A. T. (2017). *Early childhood health shocks and adult wellbeing: Evidence from wartime Britain* (NBER Working Paper 23763). Cambridge, MA: National Bureau of Economic Research.

Schwandt, H., & von Wachter, T. M. (2020). *Socioeconomic decline and death: Midlife impacts of graduating in a recession* (NBER Working Paper 26638). Cambridge, MA: National Bureau of Economic Research.

Schwartz, J. (2000). Harvesting and long-term exposure effects in the relation between air pollution and mortality. *American Journal of Epidemiology, 151,* 440–448.

Sharrow, D. J., & Anderson, J. J. (2016). Quantifying intrinsic and extrinsic contributions to human longevity: Application of a two-process vitality model to the Human Mortality Database. *Demography, 53,* 2105–2119.

Steves, C. J., Spector, T. D., & Jackson, S. H. D. (2012). Ageing, genes, environment and epigenetics: What twin studies tell us now, and in the future. *Age and Ageing, 41,* 581–586.

Strittmatter, A., Sunde, U., & Zegners, D. (2020). Life cycle patterns of cognitive performance over the long run. *Proceedings of the National Academy of Sciences, 117,* 27255–27261.

Tanner, J. M. (1981). *A history of the study of human growth.* London, UK: Cambridge University Press.

Thiele, T. N. (1871). On a mathematical formula to express the rate of mortality throughout the whole of life, tested by a series of observations made use of by the Danish Life Insurance Company of 1871. *Journal of the Institute of Actuaries, 16,* 313–329.

Toulemon, L., & Barbieri, M. (2008). The mortality impact of the August 2003 heat wave in France: Investigating the harvesting effect and other long-term consequences. *Population Studies, 62,* 39–53.

Vaupel, J. W., Manton, K. G., & Stallard, E. (1979). The impact of heterogeneity in individual frailty on the dynamics of mortality. *Demography, 16,* 439–454.

Weibull, W. (1951). Wide applicability. *Journal of Applied Mechanics, 103,* 293–297.

Wilcox, A. J., & Russell, I. T. (1983). Birthweight and perinatal mortality: I. On the frequency distribution of birthweight. *International Journal of Epidemiology, 12,* 314–318.

Wilson, N., Clement, C., Summers, J. A., Bannister, J., & Harper, G. (2014). Mortality of first world war military personnel: Comparison of two military cohorts. *BMJ, 349,* g7168. https://doi.org/10.1136/bmj.g7168

Wong, C. C. Y., Caspi, A., Williams, B., Craig, I. W., Houts, R., Ambler, A., . . . Mill, J. (2010). A longitudinal study of epigenetic variation in twins. *Epigenetics, 5,* 516–526.

Zeger, S. L., Dominici, F., & Samet, J. (1999). Harvesting-resistant estimates of air pollution effects on mortality. *Epidemiology, 10,* 171–175.

Adriana Lleras-Muney (corresponding author)
alleras@econ.ucla.edu

Lleras-Muney • Department of Economics, University of California, Los Angeles, Los Angeles, CA, USA; https://orcid.org/0000-0002-9771-8611

Moreau • International Monetary Fund, Washington, DC, USA